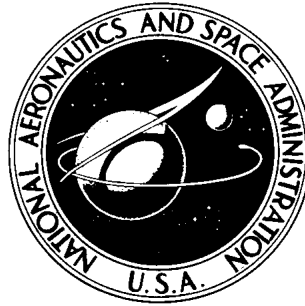


NASA TECHNICAL NOTE



NASA TN D-6297

NASA TN D-6297

**AN INVESTIGATION OF TWO VARIATIONS
OF THE GAS GENERATOR METHOD
TO CALCULATE THE THRUST OF
THE AFTERBURNING TURBOFAN ENGINES
INSTALLED IN AN F-111A AIRPLANE**

by Frank W. Burcham, Jr.

*Flight Research Center
Edwards, Calif. 93523*

1. Report No. NASA TN D-6297		2. Government Accession No.		3. Recipient's Catalog No.	
4. Title and Subtitle AN INVESTIGATION OF TWO VARIATIONS OF THE GAS GENERATOR METHOD TO CALCULATE THE THRUST OF THE AFTERBURNING TURBOFAN ENGINES INSTALLED IN AN F-111A AIRPLANE				5. Report Date April 1971	
				6. Performing Organization Code	
7. Author(s) Frank W. Burcham, Jr.				8. Performing Organization Report No. H-643	
9. Performing Organization Name and Address NASA Flight Research Center P.O. Box 273 Edwards, California 93523				10. Work Unit No. 126-15-02-02-24	
				11. Contract or Grant No.	
				13. Type of Report and Period Covered Technical Note	
12. Sponsoring Agency Name and Address National Aeronautics and Space Administration Washington, D. C. 20546				14. Sponsoring Agency Code	
15. Supplementary Notes					
16. Abstract <p style="text-align: center;">The NASA Flight Research Center investigated two variations of the gas generator method for calculating the net thrust of the afterburning turbofan engines installed in an F-111A airplane. An influence coefficient study and two ground thrust tests were performed. It was found that the gas generator method can be successfully applied to an afterburning turbofan engine. At static conditions with two engines operating, ± 2 percent accuracy can be achieved for most power settings using either the method based primarily on nozzle total pressure and area (PTA) or the method based primarily on nozzle total temperature and weight flow (TTW). For in-flight conditions the influence coefficient results indicated that the accuracy of the TTW method was about ± 3 percent, whereas the accuracy of the PTA method was about ± 5 percent for a military power setting. With either calculation method, additional errors in calculated thrust of ± 2 percent could result from high inlet flow distortion. If accurate thrust values are required, both thrust calculation methods should be used.</p>					
17. Key Words (Suggested by Author(s)) Thrust measurement Afterburning turbofan engine Gas generator method F-111A airplane			18. Distribution Statement Unclassified - Unlimited		
19. Security Classif. (of this report) Unclassified		20. Security Classif. (of this page) Unclassified		21. No. of Pages 29	
				22. Price* \$3.00	

AN INVESTIGATION OF TWO VARIATIONS OF THE GAS GENERATOR METHOD
TO CALCULATE THE THRUST OF THE AFTERBURNING TURBOFAN
ENGINES INSTALLED IN AN F-111A AIRPLANE

Frank W. Burcham, Jr.
Flight Research Center

INTRODUCTION

Many high-performance aircraft capable of efficient operation at subsonic and supersonic speeds are powered by afterburning turbofan engines. It is important to be able to accurately determine the thrust of these engines in flight so that installation losses and aircraft drag characteristics may be determined. A recent study (ref. 1) showed that the "swinging rake" method of thrust calculation is unsatisfactory for an afterburning turbofan engine because of the large gradients in pressure and temperature at the nozzle exit. Fixed exhaust sampling probes such as those used in the tests described in references 2 and 3 would undoubtedly be even less satisfactory. The gas generator method of thrust calculation offers promise for application to a turbofan engine because it does not require exhaust plane flow measurements. This method was used successfully for the afterburning turbojet engines of the XB-70A airplane (refs. 4 and 5). Two variations of the method exist: one is based primarily on exhaust nozzle total pressure and area, and the other on exhaust nozzle total temperature and weight flow.

This study was undertaken to determine the feasibility of applying the gas generator method to an afterburning turbofan engine and to compare the results of the two calculation procedures. The NASA Flight Research Center's F-111A airplane, which is powered by two TF30 afterburning turbofan engines, was instrumented to obtain the measurements required for the two variations of the method. The actual installed engine thrust was measured in two separate tests on a ground thrust calibration facility and compared with the calculated thrust values. Comparisons are presented for the full range of power settings for one and two engines operating.

An influence coefficient study was made to compare the two calculation methods. The results of this study are presented for ground static conditions and for flight conditions. A series of runs was also made with the inlet geometry positioned to generate high inlet flow velocities. These runs were used to evaluate the effects of distortion on thrust calculation accuracy. Other objectives of these runs were to obtain high response inlet pressure measurements prior to stall and to evaluate compressor noise attenuation due to inlet choking.

This report concerns only the calculation of net engine thrust. Calculation of aircraft net propulsive effort requires, in addition to net engine thrust, the propulsion

system drag terms, such as inlet additive drag, boundary-layer bleed drag, and exhaust nozzle/airframe interaction effects. These latter terms are not discussed.

SYMBOLS

The units for the physical quantities defined in this report are given in the International System of Units (SI) and parenthetically in U. S. Customary Units. Measurements were taken in U. S. Customary Units. Factors relating the two systems are presented in reference 6.

A	geometric area, m^2 (ft^2)
C_{F_g}	gross thrust coefficient
C_i	influence coefficient (See appendix.)
c	local speed of sound, m/sec (ft/sec)
D_r	relative distortion (See appendix.)
E	error in calculated net thrust, $\frac{F_{n, calc} - F_{n, meas}}{F_{n, meas}} \times 100$, percent
F_g	gross thrust, N (lb)
F_n	net thrust, N (lb)
$F_{n, calc}$	calculated net thrust, N (lb)
$F_{n, meas}$	net thrust measured by the thrust platforms, N (lb)
F_r	ram drag, N (lb)
g	conversion factor, $1 N\text{-}sec^2/kg\text{-}m$ ($32.17 ft\text{-}lb/lb\text{-}sec^2$)
K_D	distortion factor (See appendix.)
M	Mach number
NPR	nozzle pressure ratio, $\frac{p_{t, 10}}{p_\infty}$
N_1	engine low-pressure compressor speed, rpm

N_2	engine high-pressure compressor speed, rpm
p	static pressure, N/m^2 (lb/ft ²)
p_t	total pressure, N/m^2 (lb/ft ²)
R	gas constant, 286 J/kg-°K (53.34 ft-lb/lb-°R)
T	temperature, °K (°R) or °C (°F)
T_t	total temperature, °K (°R)
V	velocity, m/sec (ft/sec)
w	weight flow, kg/sec (lb/sec)
γ	ratio of specific heats
$\Delta p_{t,AB}$	difference between afterburner inlet and exit total pressure, $p_{t,7m} - p_{t,10}$
η_c	combustion efficiency
Subscripts:	
AB	afterburner
av	average value
e	engine
f	fuel flow
i	ideal
max	maximum
PTA	total pressure and area thrust calculation method
TTW	total temperature and weight flow thrust calculation method
t	total
∞	free stream
Engine station numbers (fig. 1):	
2	compressor face

- 2.6 fan discharge
- 3 low-pressure compressor discharge
- 4 high-pressure compressor discharge
- 5 turbine inlet
- 7m mixed turbine and fan discharge
- 10 primary nozzle exit
- 11 secondary nozzle exit

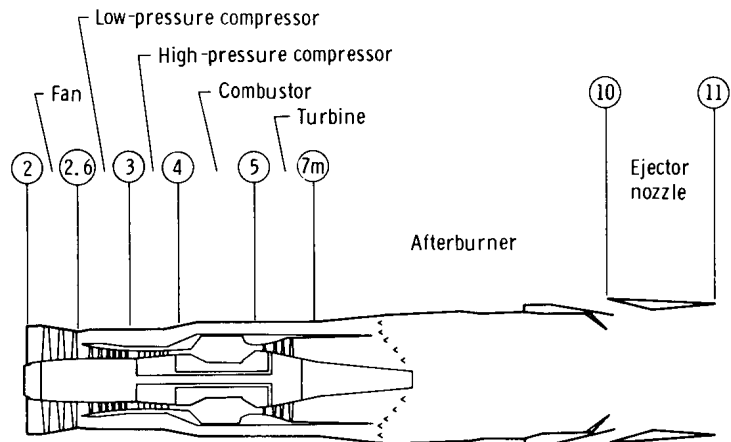


Figure 1. Schematic view of the TF30 afterburning turbofan engine with station designations.

DESCRIPTION OF TEST AIRPLANE

The F-111A airplane, S/N 639771, shown in figure 2 is a current tactical fighter with variable wing sweep. With wings fully swept, it has a Mach number capability in excess of 2.2. It is also capable of efficient cruise at subsonic speeds with the wings extended. Thrust is provided by two TF30 afterburning turbofan engines mounted side

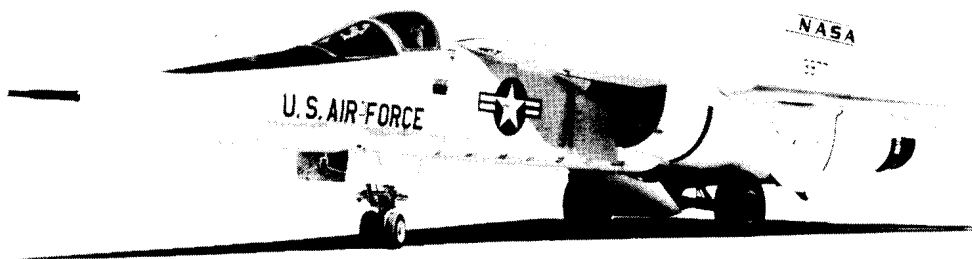
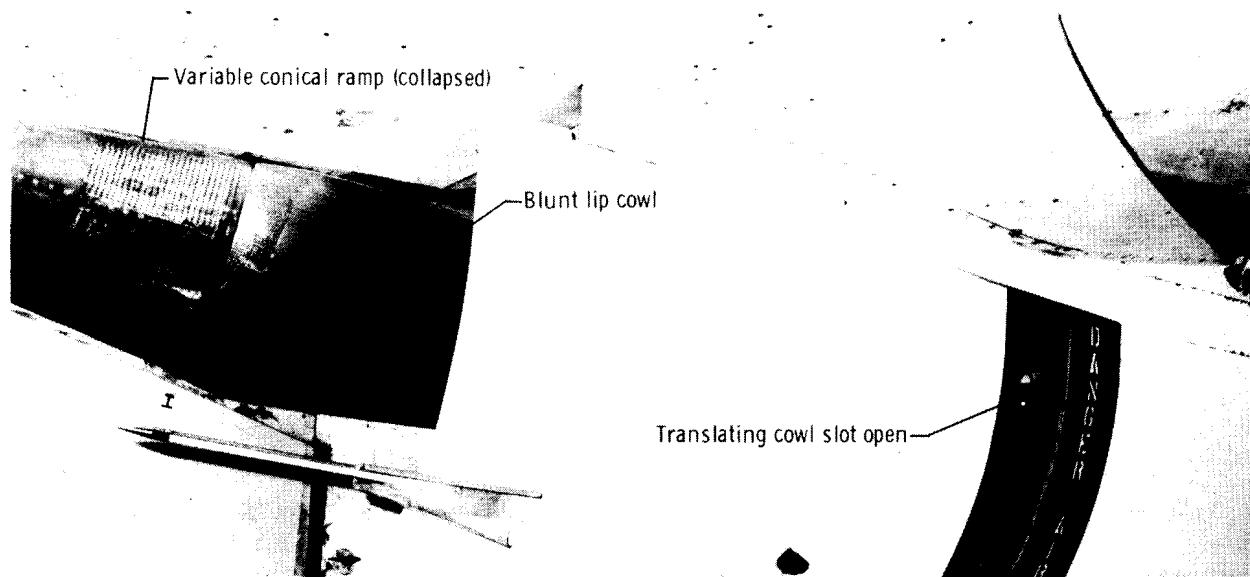


Figure 2. Photograph of the F-111A test airplane.

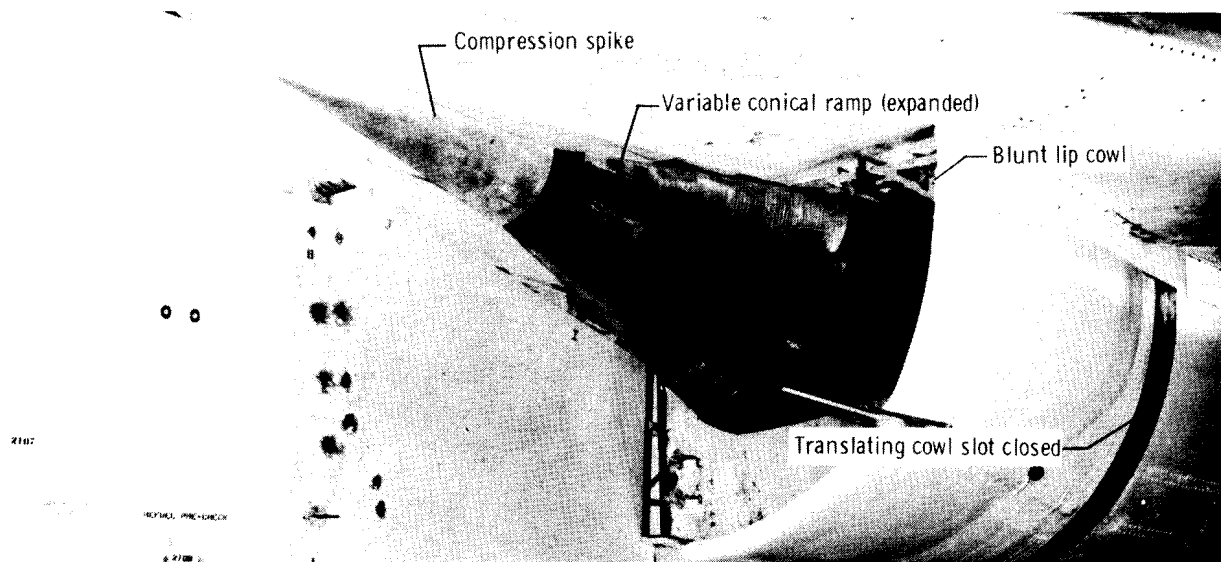
E-20273

by side in the aft fuselage. The air inlets, shown in figure 3, are one-quarter circle, external compression types mounted under the wing root. Inlet geometry can be varied by moving the compression spike forward and rearward, changing the angle of the second conical ramp, and opening the translating cowl slot.

The normal inlet configuration for static and low-speed operation is shown in figure 3(a). The second conical ramp is fully collapsed, and the translating cowl slot is open. For high inlet distortion tests, the inlet was operated off design by closing the translating cowl slot and by expanding the second conical ramp, as shown in figure 3(b).



(a) Translating cowl slot open; variable conical ramp collapsed.



(b) Translating cowl slot closed; variable conical ramp expanded.

Figure 3. Photographs of the left air inlet of the F-111A test airplane.

Two variations in the shape of the cowl lip were tested: A blunt lip cowl (fig. 3), was used for the first ground test, and a sharper cowl lip was installed for the second ground test.

DESCRIPTION OF ENGINE

The engines installed in the F-111A test airplane were Pratt & Whitney TF30-P-1 engines equipped with blow-in door ejector nozzles. The TF30 engine is in the 80,000-newton (18,000-pound) thrust class. It is a low bypass ratio engine and was the first turbofan engine to be equipped with an afterburner. Figure 1 (page 4) shows a cutaway view of the engine. A three-stage fan and a six-stage low-pressure compressor are driven at N_1 speed. A seven-stage high-pressure compressor is driven by a separate shaft at N_2 speed. Combustion takes place in an eight-chamber combustor. The turbine section consists of a single-stage turbine to drive the high-pressure compressor at N_2 speed and a three-stage turbine to drive the fan and low-pressure compressor at N_1 speed.

A fully modulating afterburner with five zones arranged in annular rings is located downstream of the turbine at the point where the core and fan streams merge. The primary nozzle at the end of the afterburner is fully closed for all nonafterburning power settings except idle. The nozzle area is variable for intermediate afterburning conditions and is fully open for maximum afterburner and idle.

An aerodynamically actuated blow-in door ejector is installed on the engine. The blow-in doors and secondary nozzle segments are positioned by pressure differential to maintain the proper expansion of the gas stream. At static conditions all six blow-in doors are in the full open position and the secondary nozzle is fully closed. More details concerning the blow-in door ejector nozzle are presented in reference 7.

The two engine exhaust nozzles are located close together at the rear end of the airplane, as shown in figure 4. During static operation, the nozzle and exhaust flows

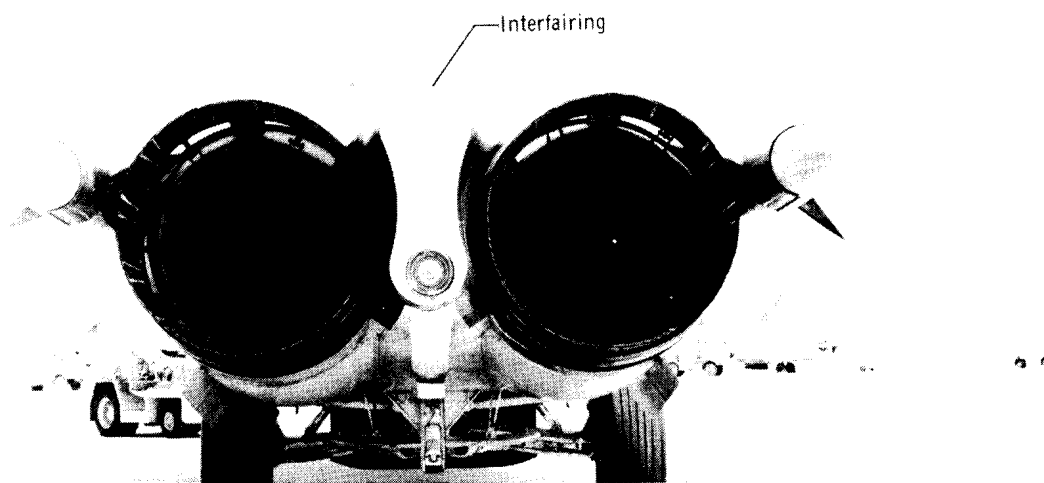


Figure 4. Photograph of the engine nozzle installation on the F-111A test airplane. E-16807

reduce the pressures on the aft airplane surfaces, particularly on the interfairing between the engines. This effect requires a correction to the measured thrust, as discussed later.

Figure 5 shows the relationship between the power lever angle and the measured static engine thrust in percent of the maximum thrust, $F_{n,max}$. The $F_{n,max}$ varied from engine to engine and from the first ground test to the second ground test, averaging about 65,000 newtons (14,500 pounds). Installation losses and the test altitude account for the reduced thrust. Thrust varies linearly with power lever angle up to military power. The figure also shows the five zones of afterburning power settings.

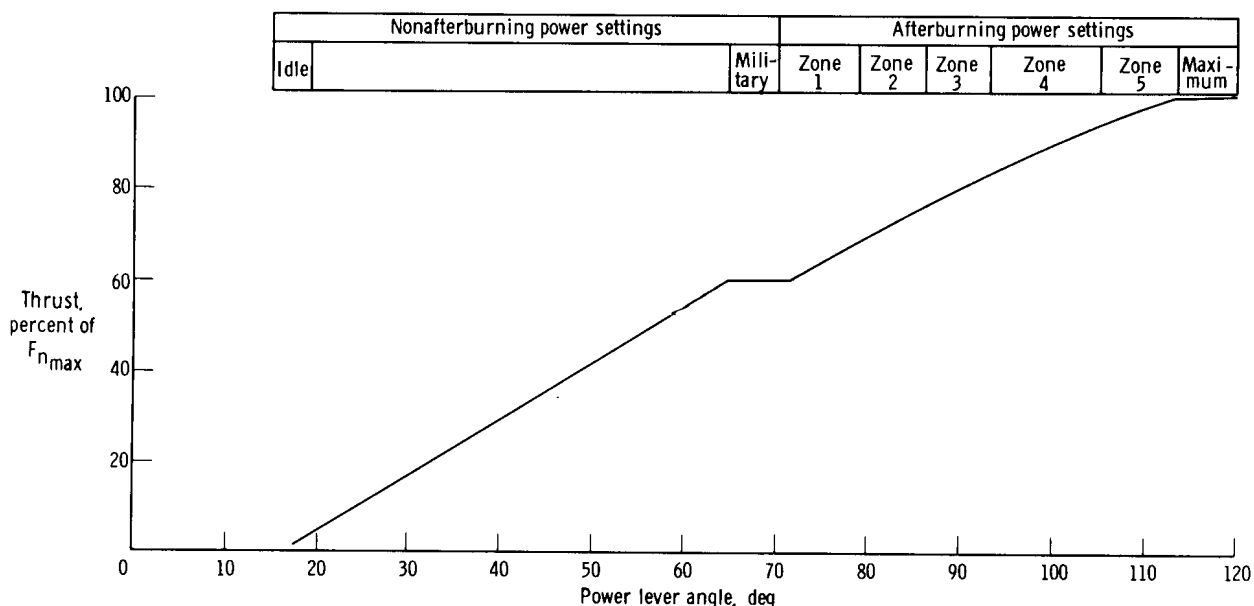


Figure 5. Relationship between power lever angle and static thrust for the TF30 engine in the F-111A test airplane.

TESTS

The thrust measurement data were obtained in two separate tests. The first test was made about 3 months before the second test. The following tabulation shows the significant differences between the two tests:

Ground test	Cowl lip configuration	Ambient air temperature, °C (°F)
1	Blunt	27 (80)
2	Sharp	4 (40)

Both tests were made during the early morning hours when winds were calm and temperature changes small. Each test was completed in about 3 hours.

The test airplane was attached to the Edwards Air Force Base static-thrust calibration facility. This facility, described in reference 5, consists of four platforms

each of which measures applied force. For these tests, the airplane was positioned with both main landing gear wheels on the center platform and the nose gear on the forward platform.

Because of the limited instrumentation in the right engine, the runs were conducted to make left and right engine conditions similar for all runs in which both engines were operating. Engine pressure ratios, $\frac{p_{t, 7m}}{p_{t, 2av}}$, were matched for nonafterburning power settings, and primary nozzle areas were matched during afterburning runs. Cowls were open for all stabilized runs. Thrust and rpm were stabilized for 1 minute at each power setting, then a 15-second data burst was taken. Data were obtained at power lever angles of idle, 20°, 30°, 40°, 50°, 60°, military, and in each of the five zones of afterburning operation with both engines operating. Runs were also made at decreasing as well as increasing thrust levels. A similar series of runs was then conducted with the right engine shut down.

At the completion of these stabilized power runs, a series of runs with gradually increasing rpm was made with the translating cowl closed. For some of these runs, the inlet spike and cone were positioned to further reduce the inlet flow area. These test conditions were used to generate high inlet distortion, inlet choking, and compressor stalls.

THRUST CALCULATION

Ideal Gross Thrust Calculation

The two thrust calculation procedures used in this study--the total temperature and weight flow (TTW) and the total pressure and area (PTA)--differ mainly in the method used to calculate the ideal gross thrust. In both methods the ideal gross thrust is defined as the thrust obtained when the flow at the primary nozzle is isentropically expanded to free-stream static pressure, that is,

$$F_{g, i} = \frac{wV_i}{g}$$

The ideal velocity, V_i , is used in both methods,

$$V_i = M_i c$$

The ideal Mach number, M_i , is a function of nozzle pressure ratio, $\frac{p_{t, 10}}{p_\infty}$, and the ratio of specific heats, γ ,

$$M_i = \sqrt{\left[\left(\frac{p_{t,10}}{p_\infty} \right)^{\left(\frac{\gamma-1}{\gamma} \right)} - 1 \right] \left(\frac{2}{\gamma-1} \right)}$$

and the local speed of sound, c , is defined by the expression

$$c = \sqrt{\gamma R T g}$$

Converting T to T_t by using $\frac{T_t}{T} = \left(\frac{p_t}{p} \right)^{\left(\frac{\gamma-1}{\gamma} \right)}$ and simplifying, the ideal velocity becomes

$$V_i = \sqrt{T_{t,10}} \sqrt{\frac{2\gamma R g}{\gamma-1}} \sqrt{1 - \left(\frac{p_{t,10}}{p_\infty} \right)^{-\left(\frac{\gamma-1}{\gamma} \right)}}$$

The ideal thrust for the TTW method is obtained by multiplying the ideal velocity by the exhaust mass flow as follows:

$$F_{g,i(TTW)} = \frac{w_{10} V_i}{g} = \frac{w_{10}}{g} \sqrt{T_{t,10}} \sqrt{\frac{2\gamma R g}{\gamma-1}} \sqrt{1 - \left(\frac{p_{t,10}}{p_\infty} \right)^{-\left(\frac{\gamma-1}{\gamma} \right)}} \quad (1)$$

Primary input parameters are airflow, total temperature, and nozzle pressure ratio.

To obtain the PTA equation, the continuity equation is used at the primary nozzle exit:

$$w_{10} = V_{10} A_{10} \frac{p_{10}}{RT_{10}}$$

For choked conditions where $M_{10} = 1.00$, substituting this expression into the TTW equation, rearranging, and simplifying results in the equation

$$F_{g,i(PTA)} = p_{t,10} A_{10} \gamma \sqrt{\left(\frac{2}{\gamma-1} \right) \left(\frac{2}{\gamma+1} \right)^{\left(\frac{\gamma+1}{\gamma} \right)}} \sqrt{1 - \left(\frac{p_{t,10}}{p_\infty} \right)^{-\left(\frac{\gamma-1}{\gamma} \right)}} \quad (2)$$

Primary inputs are $p_{t,10}$, A_{10} , and nozzle pressure ratio, NPR. The last factor in

both the TTW and PTA thrust equations is the same square root of the function of nozzle pressure ratio,

$$f(\text{NPR}) = \sqrt{1 - \left(\frac{p_{t,10}}{p_{\infty}}\right)^{-\left(\frac{\gamma-1}{\gamma}\right)}}$$

and the next to last factor in both equations is a function only of γ , or γ and R . Therefore, the two equations can be written as follows:

$$F_{g,i(\text{TTW})} = \frac{w_{10}}{g} \sqrt{T_{t,10}} f(\gamma, R) f(\text{NPR})$$

$$F_{g,i(\text{PTA})} = p_{t,10} A_{10} f(\gamma) f(\text{NPR})$$

For unchoked flow, the PTA ideal thrust can be simplified because the ideal velocity is achieved at the primary nozzle.

$$F_{g,i(\text{PTA})} = p_{\infty} A_{10} \left(\frac{2\gamma}{\gamma-1}\right) \left[\left(\frac{p_{t,10}}{p_{\infty}}\right)^{\frac{\gamma-1}{\gamma}} - 1 \right] (\text{unchoked})$$

The nozzle pressure ratio factor is to the first power for the unchoked condition.

Gross Thrust Coefficients

Ideal thrust is converted to actual thrust by using a gross thrust coefficient, C_{F_g} , which is determined from engine test cell runs and model tests. The gross thrust coefficient at static conditions is determined in a test facility by measuring the actual thrust, calculating the ideal thrust, and lumping all the differences into the gross thrust coefficient:

$$C_{F_g} = \frac{F_g}{F_{g,i}}$$

This term accounts for such factors as blow-in door and ejector forces, nonisentropic expansion, friction, nonaxial flow, nozzle leakage, and differences between geometric and effective flow areas. For flight conditions, scale models are used to account for external flow effects. Isolated ejector tests and small-scale complete model tests are used. A more complete description of this coefficient is included in reference 7. For the PTA method, the gross thrust coefficient includes a discharge coefficient to relate the measured geometric nozzle area to the effective flow area. The TTW method does not require this term, however. The actual gross thrust equations for

the two methods are as follows:

$$F_{g(PTA)} = F_{g,i(PTA)} C_{Fg(PTA)}$$

$$F_{g(TTW)} = F_{g,i(TTW)} C_{Fg(TTW)}$$

Ram Drag and Net Thrust

For both methods ram drag is calculated from airflow and free-stream velocity by using the expression

$$F_r = \frac{w_2}{g} V_\infty$$

The final equations for net thrust are (for choked conditions) as follows:

$$F_{n(PTA)} = \left[p_{t,10} A_{10} f(\gamma) f(NPR) \right] C_{Fg(PTA)} - \frac{w_2 V_\infty}{g} \quad (3)$$

$$F_{n(TTW)} = \left[\frac{w_{10}}{g} \sqrt{T_{t,10}} f(\gamma, R) f(NPR) \right] C_{Fg(TTW)} - \frac{w_2 V_\infty}{g} \quad (4)$$

One important fact should be noted. Weight flow appears in both the gross thrust and the ram drag terms of the TTW equation, thus errors due to weight flow measurement inaccuracies should be partially canceled.

Calculation Procedures

The PTA calculation procedure is described in detail in reference 7. Also described are many of the engine characteristics, such as airflow versus corrected rpm, afterburner pressure drop, and nozzle gross thrust coefficients, which are used in both calculation procedures.

The TTW calculation procedure is similar to that described in references 4 and 5 and is based on an energy balance through the engine. Available energy is increased by the burning of fuel and is decreased because of horsepower extraction, bleed air extraction, and inefficiencies in the compressors, burners, and nozzle. Extensive data defining the performance characteristics of the various components of the engine, such as compression and combustion efficiencies and pressure losses, are required to perform the TTW calculation. Some of the data were available from the PTA method, and some were obtained from TF30 engine tests performed in an altitude

TABLE 1. — PARAMETERS, RANGES, AND ACCURACIES OF THRUST DETERMINATION MEASUREMENTS

Parameter	Number of measurements	Range	Percent of full-scale accuracy
p_{∞}	1	5 to 100 kN/m ² (100 to 2100 lb/ft ²)	±0.3
$T_{t\infty}$	2	220 to 480° K (400 to 860° R)	±.5
$p_{t,2}(\text{hub})$	2	0 to 200 kN/m ² (0 to 4320 lb/ft ²)	±2
^a $p_{t,2}$	20	±70 kN/m ² (±1440 lb/ft ²)	±2
^a p_2	8	±40 kN/m ² (±860 lb/ft ²)	±2
$p_{t,2.6}$	8	34 to 345 kN/m ² (720 to 7200 lb/ft ²)	±2
$p_{2.6}$	1	34 to 345 kN/m ² (720 to 7200 lb/ft ²)	±2
p_3	1	34 to 1100 kN/m ² (720 to 23,000 lb/ft ²)	±2
p_4	1	0 to 3450 kN/m ² (0 to 72,000 lb/ft ²)	±2
Power lever angle	2	0 to 120°	±2
N_1	2	0 to 11,000 rpm	±1
N_2	2	0 to 17,000 rpm	±1
$T_{t,5}$	2	0 to 1600° K (0 to 2880° R)	±2
$p_{t,7m}(\text{low range})$	2	0 to 170 kN/m ² (0 to 3600 lb/ft ²)	±1
$p_{t,7m}(\text{high range})$	2	0 to 275 kN/m ² (0 to 5760 lb/ft ²)	±1
$w_{fe}(\text{volumetric})$	2	0.45 to 7.5 $\frac{\text{m}^3}{\text{hr}}$ (120 to 1980 $\frac{\text{gal}}{\text{hr}}$)	±2
$w_{ft}(\text{volumetric})$	2	4.5 to 34 $\frac{\text{m}^3}{\text{hr}}$ (1200 to 9000 $\frac{\text{gal}}{\text{hr}}$)	±2
Fuel temperature	4	0 to 350° K (0 to 600° R)	±2
$w_{ft}(\text{mass})$	2	59 to 135 $\frac{\text{kg}}{\text{min}}$ (130 to 960 $\frac{\text{lb}}{\text{min}}$)	±2
A_{10}	2	0.35 to 0.66 m ² (3.76 to 7.05 ft ²)	±2
^a $p_{10}(\text{base})$	2	±70 kN/m ² (±1440 lb/ft ²)	±2
^a Interfiring static pressure	20	±70 kN/m ² (±1440 lb/ft ²)	±2

^aDifferential pressures; reference pressure accuracy approximately ±0.5 percent.

face total pressure, $p_{t,2_{av}}$, was measured on the left engine with 20 probes. Four

compressor face rakes, each with five probes positioned to sample equal areas, were used. Eight compressor face static pressures were also measured. Low and high compressor rotor speeds (N_1 and N_2) were measured on both engines by tachometers.

Fuel flow measurement is important, particularly for the TTW method. Two types of fuel flow measurements were made successfully on the F-111 airplane. The airplane had the production mass fuel flow measurement system which measures the total fuel flow to the engine and afterburner. A volumetric measuring system was added to both engines. One meter measured the total flow to both the engine and the afterburner, and another measured the flow only to the engine. The meters were each calibrated in a flow calibration facility before they were installed in the airplane. The volumetric total flowmeters were calibrated with the aircraft fuel lines upstream of the meter to simulate the aircraft installation. The volumetric meters also required a fuel temperature measurement to permit a conversion to mass flow. The total fuel flow meters operated below their calibrated range for most nonafterburning power settings; hence, the volumetric engine fuel flow reading was used exclusively. For

higher fuel flows, both the volumetric and mass total fuel flows agreed so well that either measurement could be used.

Turbine discharge pressure, $p_{t,7m}$, is an important engine measurement. The test engine is equipped with a production $p_{t,7m}$ system (ref. 7) consisting of six rakes. These rakes sample the fan stream and the core stream with an integrating rake, and all six integrated rake pressures are manifolded. This mixed average pressure is measured by two pressure transducers, one ranged for low pressures and another for higher pressures. Transducer temperatures were also measured to permit transducer temperature compensation.

Primary nozzle area, A_{10} , is determined by a production system (ref. 7) which is calibrated in terms of a nozzle actuator stroke position. Temperature effects are minimized by use of temperature-compensated cables in the measurement system. The nozzle itself is constructed in such a manner that temperature changes do not change the flow area significantly. This measurement system was calibrated twice and gives reasonably accurate results.

A large number of pressure and position measurements were made on the blow-in door ejector nozzle. Of primary importance to the thrust calculation was the measurement of the base pressure acting on the primary nozzle. Surface static pressures were also measured on the airplane interfairing and boattail region.

Ambient free-stream pressure and temperature measurements were made with the calibrated F-111 airspeed system. Power lever angle was also measured. Several other measured parameters, such as $p_{t,2.6}$, $p_{2.6}$, p_3 , p_4 , $T_{t,5}$, and p_2 , were used in the TTW calculation procedure only for comparison with the calculated values.

Data from the various measurements were digitally recorded by a pulse code modulation system. Before the data were reduced, pre-test and post-test zero corrections and power supply voltage corrections were made. Data for the stabilized thrust settings were obtained by averaging several data samples for each parameter.

ACCURACY

In a thrust calculation the overall accuracy of the final result is of great importance and is usually difficult to determine. One useful technique for assessing the accuracy of the calculation is to compute influence coefficients for important parameters. The influence coefficient of a parameter can then be multiplied by the estimated accuracy of that parameter to determine its effect on the overall thrust. By combining all the important parameters in this manner, using a root-sum-square technique, an estimate of the overall accuracy is obtained.

Influence coefficients were calculated by increasing a given parameter in the computer program by 1 percent and calculating the percentage change in the net engine thrust. These influence coefficients were calculated for the ground thrust

measurement conditions, and, by using measured flight data, were calculated for representative flight conditions from $M_\infty = 0.5$ to 2.2. It was found that in-flight influence coefficients were nearly independent of flight conditions if extreme conditions such as very low power settings at supersonic speeds were not included.

In addition to the obvious engine measurements, there are other important parameters in thrust calculation. The engine characteristics defined in the computer program are subject to some error and represent an average engine. Their influence coefficients must therefore be considered in an assessment of overall thrust accuracy. Influence coefficients for free-stream parameters such as Mach number, static pressure, and total temperature must also be considered.

The accuracy of the important input parameters to the thrust program must also be determined. Table 2 shows the estimated accuracies of the three important types

TABLE 2. - ESTIMATED ACCURACY OF KEY INPUT PARAMETERS TO THE THRUST CALCULATION PROGRAM FOR STATIC AND FLIGHT CONDITIONS

Type of parameter	Parameter	Estimated accuracy, percent	
		Static	In flight
Engine measurements	$P_{t,7m}$	0.5	1.0
	$P_{t,2av}$	1.0	2.0
	w_{fe}	1.0	1.0
	w_{ft}	1.0	1.0
	$A_{10}(\text{maximum or minimum})$.5	.5
	$A_{10}(\text{intermediate})$	2.0	2.0
Engine characteristics	η_{c_e}	1.0	1.0
	$\eta_{c,AB}$	2.0	2.0
	w_2	2.0	2.0
	$\Delta p_{t,AB}$	2.0	2.0
	C_{F_g}	1.0	1.0
Free-stream measurements	P_∞	0.25	0.50
	T_{t_∞}	.5	1.0
	M_∞	0	1.0

of input parameters for ground thrust run conditions and flight conditions. The measured engine parameter accuracies were obtained from the values in table 1, in some instances modified to account for repeatability, temperature compensation, redundant measurements, or special knowledge of the measurement. Accuracy of the engine characteristics is based primarily on scatter in the TF30 test cell data and experience with other engines. Free-stream parameter accuracies were determined from a previously obtained airspeed calibration. Certain parameters were more accurately known for the ground runs than for the flight conditions because of the stabilized and well-known environmental conditions.

The accuracy of the thrust stand force measurements must also be considered. Reference 5 specifies an accuracy of ± 450 newtons (± 100 pounds) for asymmetric loading. However, for the nearly symmetric loading applied by the F-111A airplane, and from thrust stand zero shifts, the accuracy for these tests is believed to be ± 225 newtons (± 50 pounds). This error is nearly negligible for power lever angles above about 30° , but is as much as ± 8 percent of the single-engine idle thrust. Errors in the data at power settings below 30° may be due in part to the thrust stand errors.

RESULTS AND DISCUSSION

Influence Coefficients

Influence coefficients calculated by determining the percent change in net thrust for a 1-percent increase in important parameters in both methods of calculation are shown in figures 7, 8, and 9 for ground static and flight conditions.

Measured engine parameter. — Figure 7 shows the influence coefficients for important measured engine parameters plotted as a function of power lever angle for

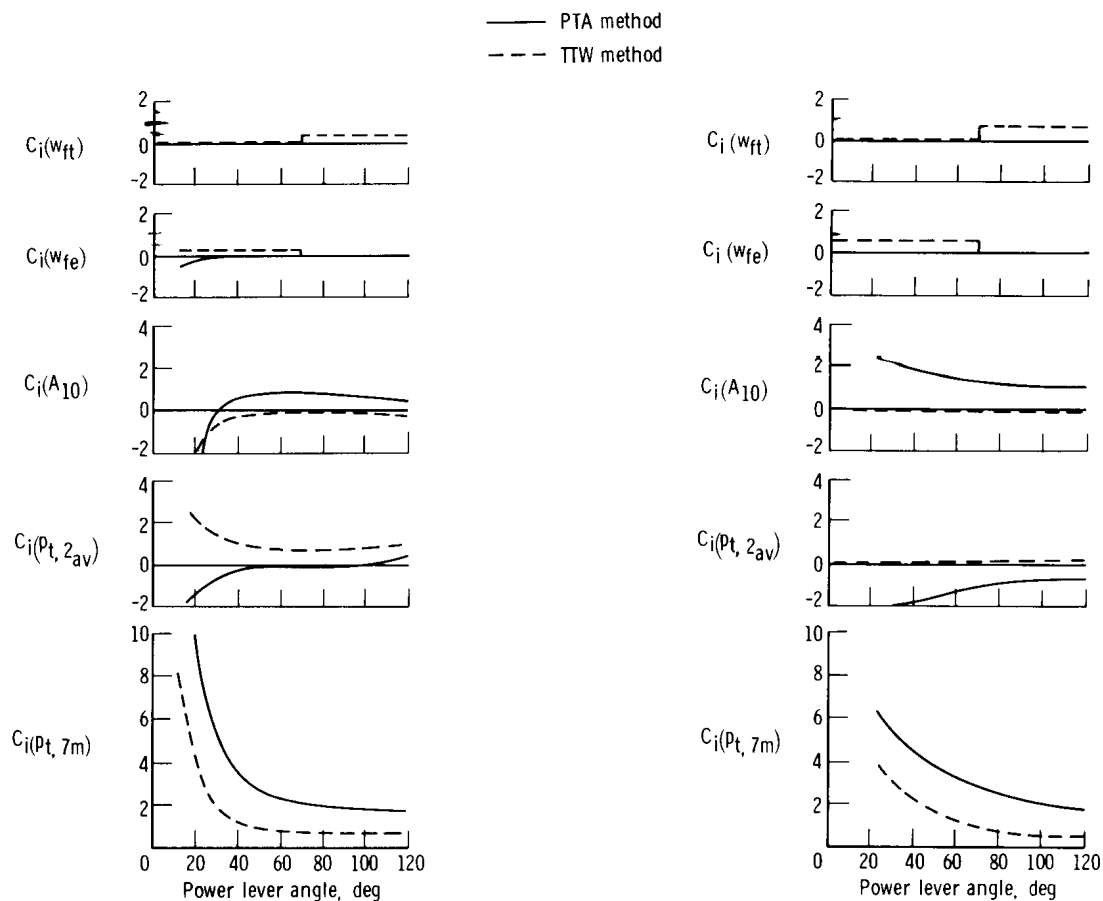


Figure 7. Effect of a 1-percent increase in important measured engine parameters on net thrust.

both the PTA and TTW calculation methods. A discontinuity in the fuel flow influence coefficients occurs between afterburning and nonafterburning power settings. In most instances, these parameters are increasingly sensitive as power lever angle is reduced, particularly the turbine discharge pressure. At static conditions (fig. 7(a)), the TTW method is more sensitive to $p_{t,2av}$, w_{fe} , and w_{ft} , and the PTA method is more sensitive to $p_{t,7m}$ and A_{10} . For flight conditions, the influence coefficients are generally somewhat larger than for the static conditions for both calculation methods, except for $p_{t,2av}$. For $p_{t,2av}$ the PTA method sensitivity increases markedly, but the TTW sensitivity is sharply reduced. This reduction in TTW sensitivity to $p_{t,2av}$ in flight is attributed to the ram drag effect shown in equation (4). There is a direct relationship between $p_{t,2av}$ and engine airflow. An error which increases the calculated airflow causes an increase in calculated TTW gross thrust and a partially compensating increase in calculated ram drag. The net thrust, then, is only slightly affected by an airflow error. The gross thrust in the PTA method is only slightly affected by airflow, but an error in airflow measurement affects the ram drag and thus the net thrust. The favorable reduction of thrust errors due to airflow errors in the TTW method does not occur at static conditions because the ram drag is zero.

Engine characteristics.—Several important engine characteristics are needed to calculate the net thrust. These characteristics are determined in ground facility tests with instrumented engines or test rigs and are representative of an average engine which may not accurately represent a particular engine because of normal engine-to-engine tolerances. Therefore, it is necessary to consider errors in parameters such as engine airflow, main and afterburner combustion efficiency, afterburner pressure loss, and nozzle gross thrust coefficient. Influence coefficients for these parameters are shown in figure 8. For static conditions (fig. 8(a)) the PTA method is more sensitive to afterburner pressure drop errors, and the TTW method is more sensitive to airflow and main burner and afterburner combustion efficiency. Gross thrust coefficient errors affect both methods equally.

For flight conditions (fig. 8(b)) the trends are all similar except for airflow, where again the ram drag effect makes the TTW method less sensitive to airflow errors than the PTA method. The influence coefficient for C_{F_g} is large. Accurate determination of C_{F_g} may be difficult for configurations such as that of the F-111 airplane in which the propulsion system interacts strongly with the airframe. It is obvious that relatively small C_{F_g} errors can make large net thrust errors, particularly at lower power settings.

Free-stream parameters.—Errors in measurement of certain free-stream parameters such as static pressure, total temperature, and Mach number can have a significant effect on calculated net thrust, as shown in figure 9. Static pressure influence coefficients become very large at low power settings because of their effect

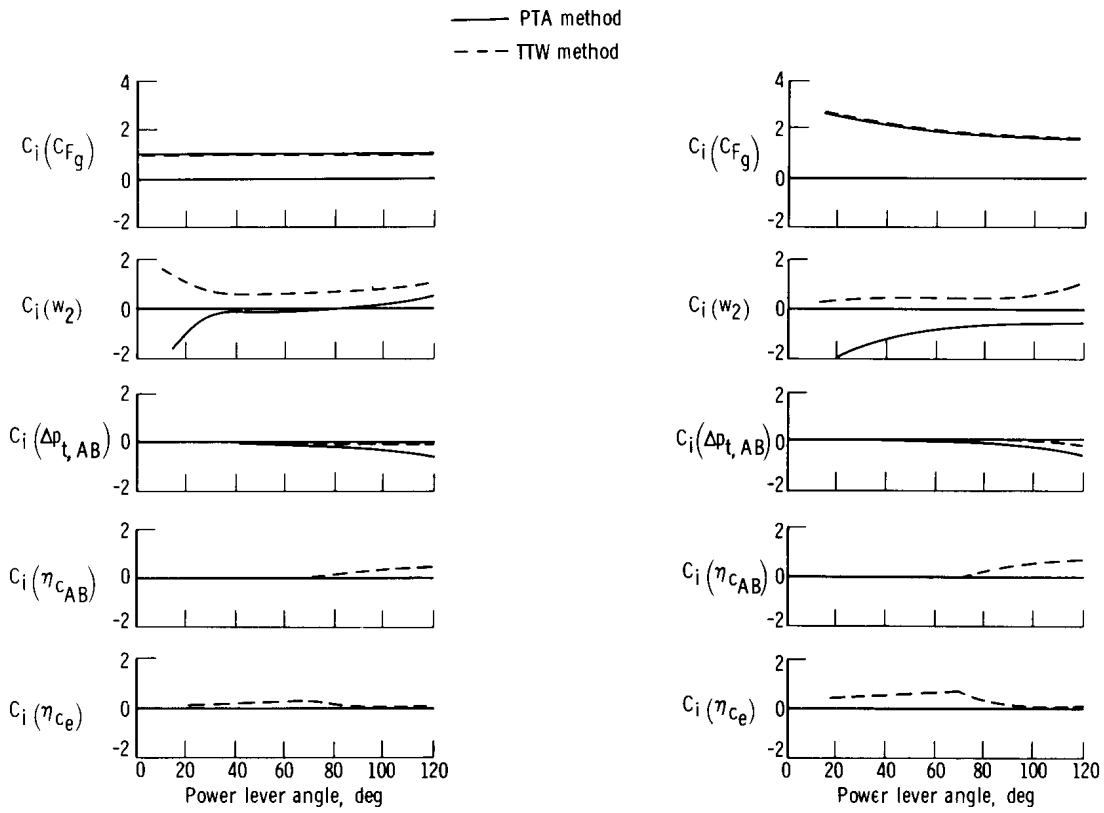


Figure 8. Effect of a 1-percent increase in important engine characteristics on net thrust.

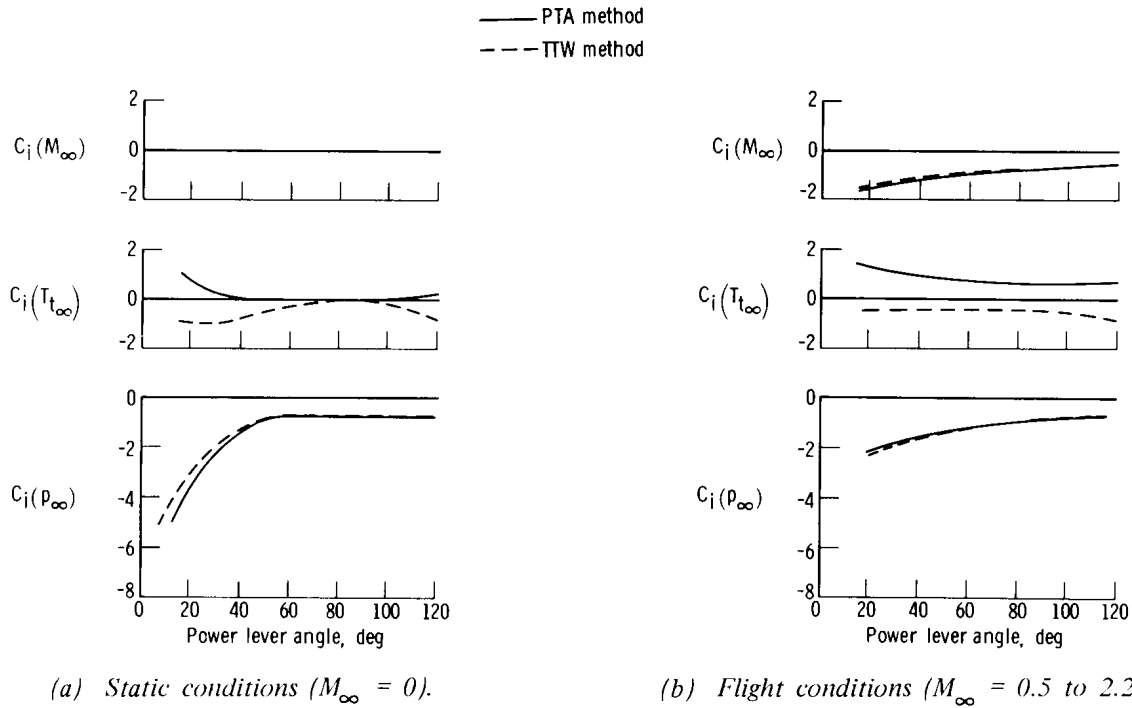


Figure 9. Effect of a 1-percent increase in important measured free-stream parameters on net thrust.

on nozzle pressure ratio, $\frac{P_{t,10}}{p_\infty}$, at both static (fig. 9(a)) and flight (fig. 9(b)) conditions. Total temperature errors are significant because increasing total temperature decreases calculated airflow. Airplane Mach number is also an important parameter in flight, primarily because of its effect on ram drag. A careful calibration of the airspeed system is essential for good thrust measurements.

Calculated Thrust Accuracy

By using the influence coefficients in figures 7, 8, and 9 and the estimated parameter accuracies from table 2, it is possible to estimate the overall thrust calculation accuracy, based on a root-sum-square combination of all the variables. Figure 10 shows this estimate. The results for the static conditions (fig. 10(a)) show that the PTA and TTW methods are approximately equal in overall accuracy, with the TTW method somewhat better at low power settings and the PTA method better at the highest power settings. Accuracy for either method approaches ± 2 percent for the higher power settings.

The data for the flight conditions (fig. 10(b)) show a clear superiority for the TTW method, primarily because of the favorable airflow error effects mentioned previously. The flight results are less accurate than the ground test results. For military power, the accuracy of the TTW method is approximately ± 3 percent, whereas the accuracy

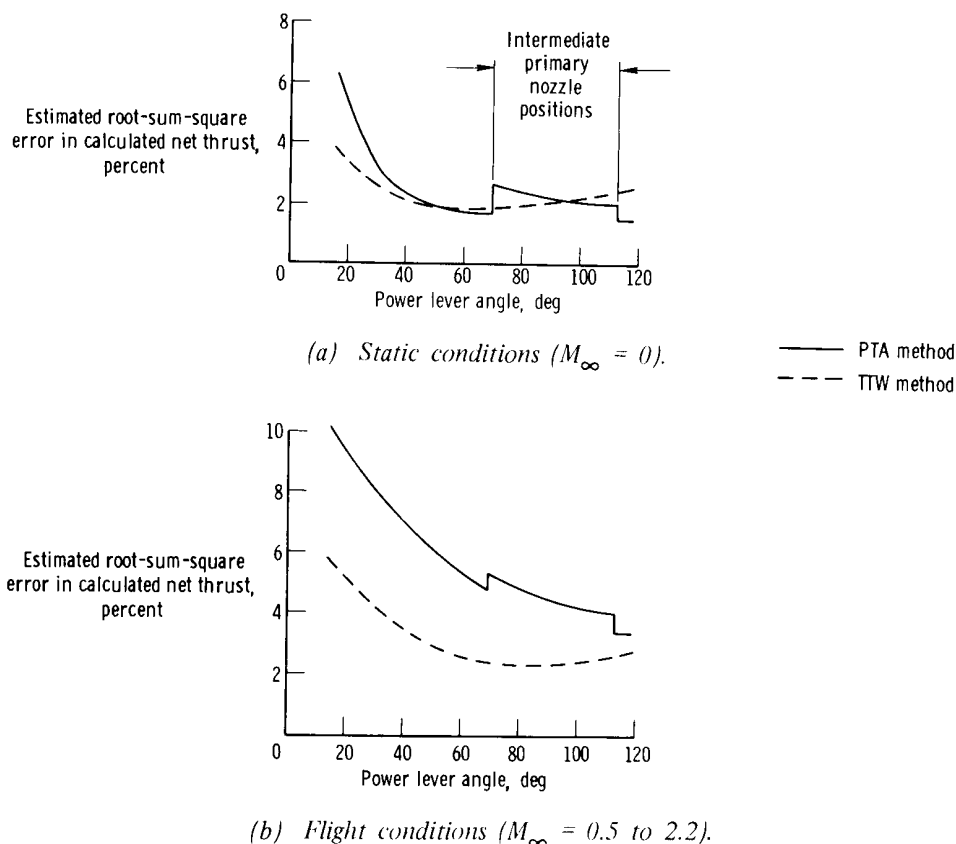


Figure 10. Root-sum-square error in calculated net thrust as estimated from influence coefficient and parameter accuracy.

of the PTA method is approximately ± 5 percent. These flight estimates are based on a ± 1 -percent error in C_{F_g} . Larger errors in C_{F_g} would cause a corresponding increase in the error in calculated thrust.

Ground Run Results

The errors between the calculated and the measured net thrust for the two ground tests are compared in figures 11 and 12. For ground test 1 with both engines operating (fig. 11(a)), the thrust calculated by the PTA method is considerably higher than measured thrust at low power settings. As power setting increases, the error or difference between the calculated and measured thrust decreases to less than 1 percent at military power and becomes negative with further increases in thrust, reaching a -3 percent error at maximum afterburner. The TTW method shows about the same trend in reverse except that the error at maximum afterburner is less than 2 percent. Maximum scatter for either method is about ± 1 percent.

When only the left engine is operating (fig. 11(b)), the trends are similar to the results for the two engines except that scatter and error increase, particularly for the TTW method at afterburning power levels, where the error approaches 4 percent.

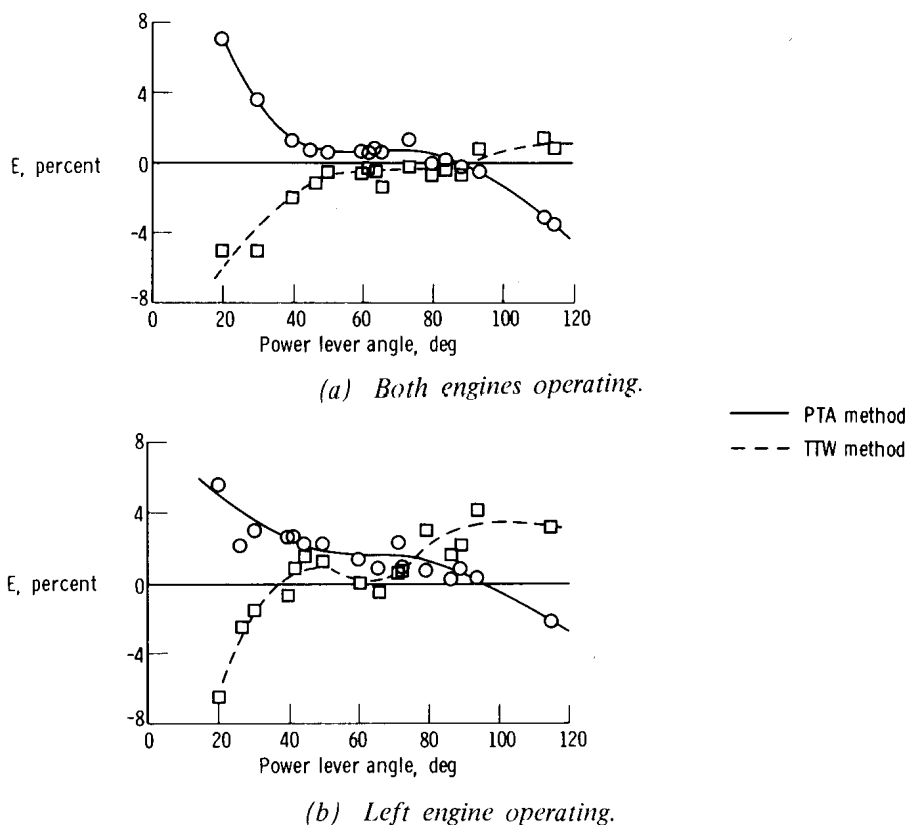


Figure 11. Effect of power lever angle on error in calculated net thrust. Ground test 1.

Figure 12 shows the same types of data for ground test 2. The results are similar to the data from ground test 1, except that the calculated thrust is about 1 percent higher for ground test 2 for both methods.

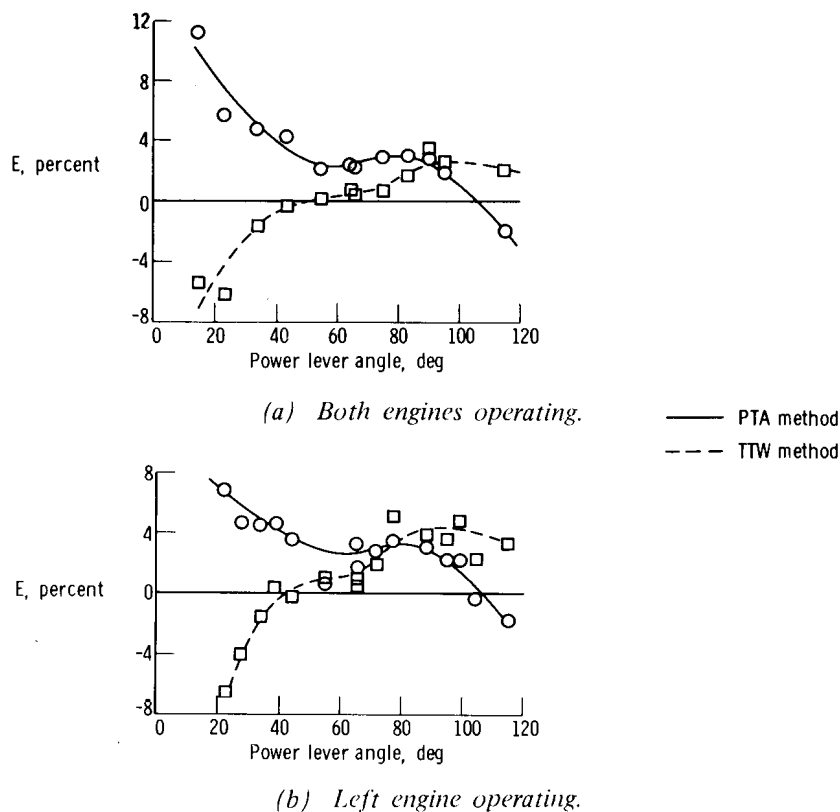


Figure 12. Effect of power lever angle on error in calculated net thrust. Ground test 2.

Figure 13 compares faired data from ground tests 1 and 2. The trends for the two tests are the same, and the trends for the two calculation procedures are almost opposite. The error in thrust is less than ± 4 percent for each method for power lever angles above 40° . For both engines operating, at military power, the accuracy is about ± 2 percent for both calculation methods. The calculation error is most repeatable in the intermediate power range, particularly for the TTW method. Repeatability is reduced for both methods for afterburning thrust levels.

The differences in the data for ground tests 1 and 2 are probably caused by deterioration of the left engine between the two tests, although the large ambient air temperature difference between tests could also be a factor. The left engine was removed shortly after the second ground test because of reduced compressor stall margin. The change of the cowl lip shape between tests caused only minor changes in compressor face recovery and distortion and is not believed to be a significant factor.

The consistency of the calculated thrust error indicates that bias errors, not random errors, make the largest contribution to the overall calculation error. This indicates a need for better engine characteristics data and more instrumentation. The opposite nature of the errors in the two methods introduces the possibility of identifying the probable error sources by looking for influence coefficients that cause opposite errors in the two methods. Errors in $P_{t,2_{av}}$ or airflow at low power settings cause

opposite and nearly equal errors similar to those in figure 13. This may explain the increase in error as power setting is reduced toward idle.

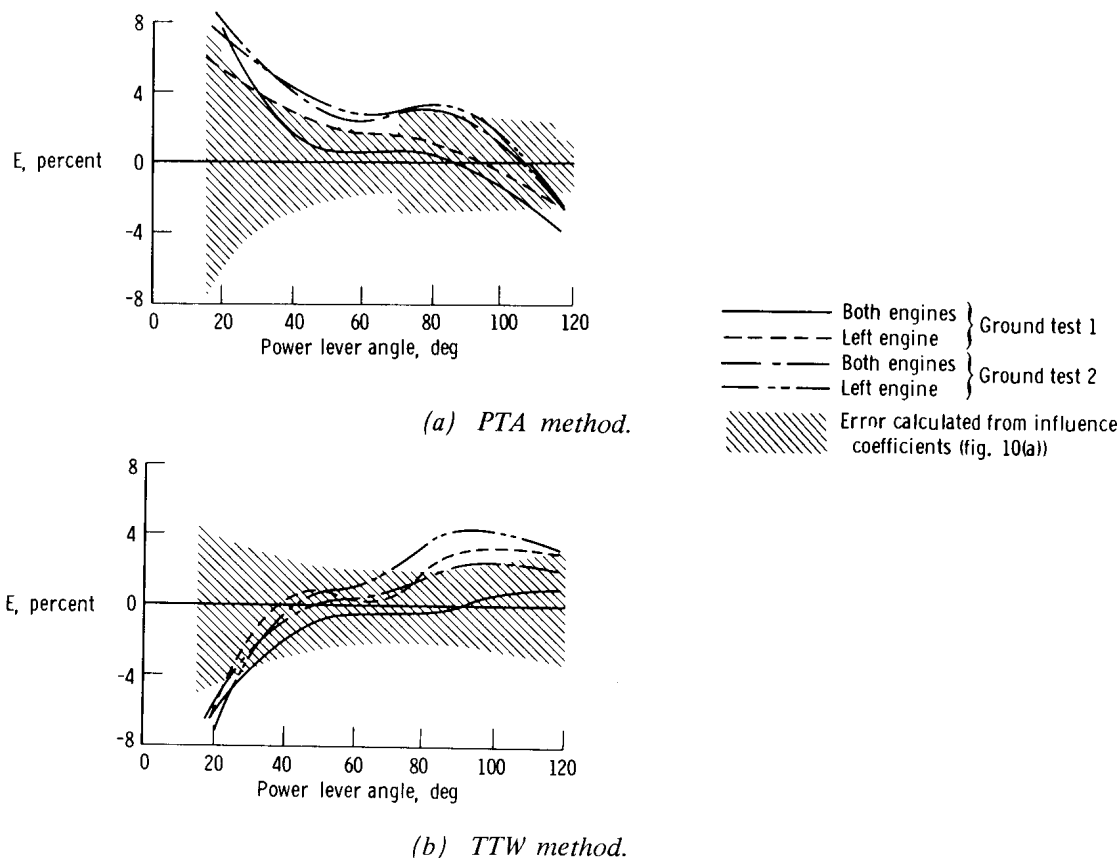


Figure 13. Effect of power lever angle and number of engines operating on faired values of calculated thrust error. Ground tests 1 and 2.

The increase in the thrust error in the TTW method for afterburning power is likely caused by an error in the assumed afterburner combustion efficiency. As noted previously, the combustion efficiency data were not available for the TF30 engine, so available data from a different engine, an afterburning turbojet, were used.

The increasing negative error in the thrust calculated by the PTA method at maximum power is probably caused by a parameter which has only slight effect on the TTW thrust error. Such a parameter could be A_{10} , $\Delta p_{t, AB}$, or $p_{t, 7m}$.

It is of interest to compare the estimated thrust error from the influence coefficients (shaded area in fig. 13) with the actual measured errors. For the PTA method (fig. 13(a)) the measured errors are generally within the estimated error band except at low power settings and maximum thrust. The TTW method measured results (fig. 13(b)) are generally within the estimated error band except for the left engine intermediate afterburning thrust levels. These results indicate the usefulness of estimated thrust accuracies based on influence coefficients and estimated parameter accuracies.

Several thrust calculations were performed during periods of nonstabilized engine operation. The results from these calculations showed little deviation from the stabilized operation results. However, the rates of change of thrust were not rapid.

Effect of Inlet Flow Distortion on Thrust Calculation Accuracy

As mentioned in the TESTS section, a series of runs was made with the inlet translating cowl closed. Cowl lip rake measurements showed high flow velocities at the inlet cowl lip and local separation. This separation caused large increases in steady-state distortion at the compressor face. With the inlet cone expanded (fig. 3(b)), sonic or near-sonic flow existed at the inlet throat and distortion increased further. Numerous compressor stalls occurred as a result of these conditions. It is of interest to investigate the effects of these highly distorted inlet conditions on the thrust calculation accuracy, particularly because in-flight distortion levels in the F-111A airplane are relatively high at some flight conditions.

Thrust calculations were performed for 21 off-design inlet situations, including 11 in which thrust data were obtained immediately before a compressor stall. Power lever angles ranged between 30° and 70°. Distortion parameter values for these conditions are plotted in figure 14 against the corrected engine airflow. Also shown is a K_D band that covers the data for the cowl-open, stabilized engine operation. The K_D values which caused compressor stall were about twice as high as the cowl-open K_D values. Intermediate K_D values between the cowl-open and compressor stall regions were obtained with various intermediate settings of the inlet geometry.

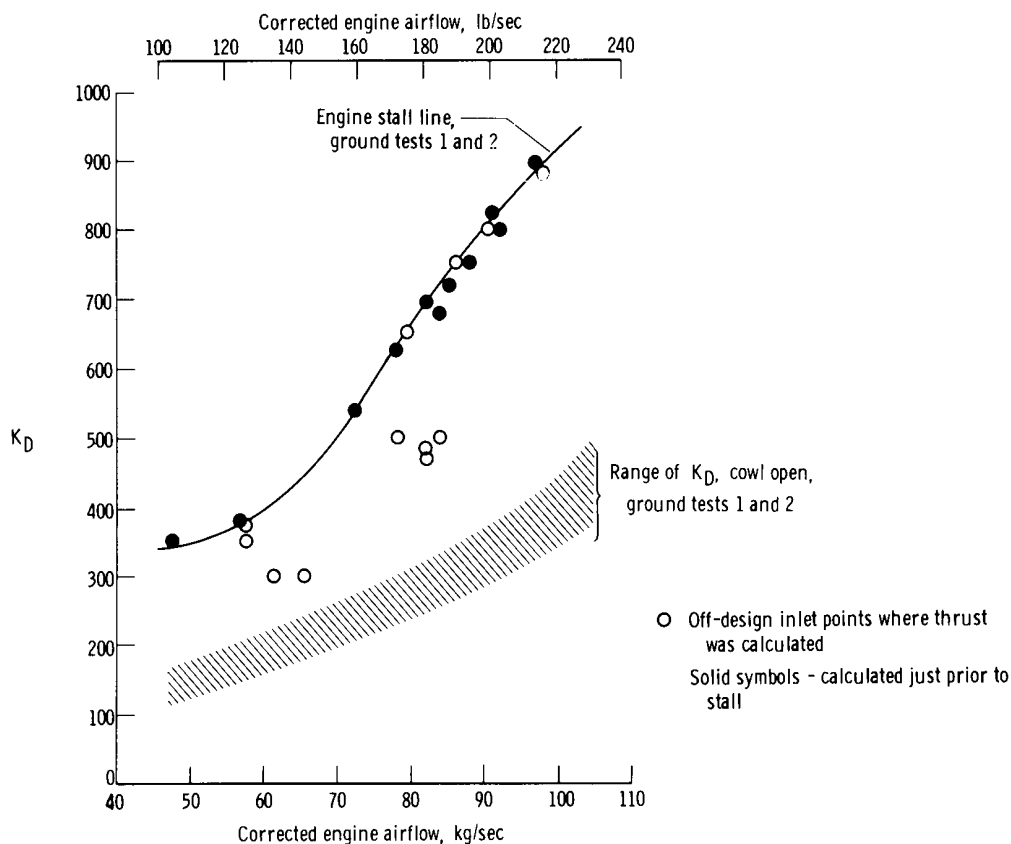


Figure 14. Effect of corrected engine airflow on distortion for off-design inlet conditions for which thrust was calculated.

Thrust values were calculated for these highly distorted conditions and compared with the measured thrust. The errors for the high distortion data were then compared with the errors for the low distortion, cowl-open data at the same thrust. The differences are plotted in figure 15 against relative distortion, D_r , which is the K_D value at that condition divided by the K_D value for the cowl-open condition at the same net thrust. For both the PTA method (fig. 15(a)) and the TTW method (fig. 15(b)), as the relative distortion increases, the range of difference between the thrust calculated with low distortion and that calculated with high distortion increases considerably. The scatter is somewhat greater for the TTW method than for the PTA method.

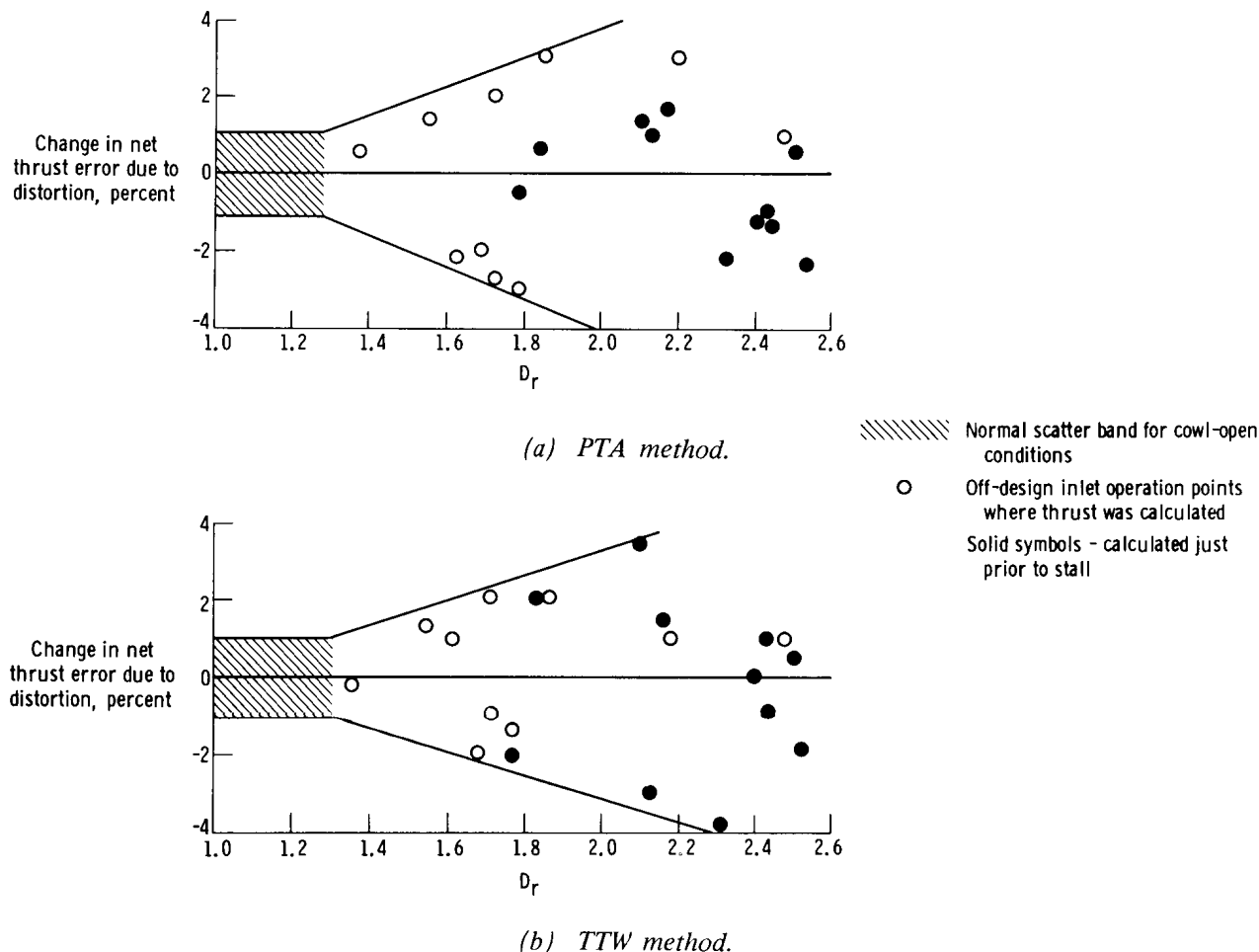


Figure 15. Effect of relative distortion on the change in calculated net thrust error for power lever angles between 30° and 70° .

It might be expected that the highly distorted inlet conditions would result in reduced compressor efficiency, pressure rise, and airflow, and that the calculated airflow would therefore be too high. This would result in the TTW calculated thrust being high, with little effect on the PTA calculated thrust. However, the data in figure 15 show essentially random scatter for both methods with possible additional thrust errors of as much as ± 2 percent for D_r values greater than about 1.6.

A possible source of error is the $p_{t,7m}$ measurement. A recent study (ref. 10)

on a nonafterburning version of the TF30 engine has shown that rather severe radial and circumferential pressure gradients exist at the turbine discharge station, even with no inlet flow distortion. The distortion effects could cause significant changes in these pressure gradients with resulting changes in the $p_{t,7m}$ measurement. The study also showed that, at some conditions, the integrating rake does not indicate the mixed average total pressure of the fan and core streams.

Additional Considerations

Aside from the analytical considerations discussed in this report, other factors must be considered in the use of the TTW and PTA methods. For instance, the fuel flow measurements that are of great importance to the TTW method may be difficult to make accurately. In the F-111A tests, the fuel flow meters were calibrated carefully, using the actual aircraft fuel lines, and the redundant total fuel flow meters were used to assure accurate fuel flow measurements. However, similar techniques were used with the XB-70 airplane (ref. 5), but fuel flow accuracy problems were never completely resolved. Fuel flow measurement accuracy on the F-111A airplane may be particularly easy to achieve.

Primary nozzle area measurement, critical to the PTA method, is another example of a problem that may vary widely in difficulty from one engine to another. In the YJ93 engine installed in the XB-70 airplane, primary nozzle area was measured by both an actuator stroke position and a pucker string length. Neither system was particularly accurate, probably because of the difficult environment. Errors in excess of ± 2 percent were common. In addition, the primary nozzle was generally not on the physical stops of maximum or minimum area. In the TF30 engine, however, the nozzle is either fully open or fully closed for all power settings except intermediate afterburning, and the nozzle area measurement proved to be considerably more accurate than that for the YJ93 engine. The decision on which calculation method is more accurate depends on the particular engine and aircraft for which it is used. However, in a test program in which accurate results are required, both methods should be used to minimize the effects of instrumentation errors and to provide a check calculation.

CONCLUSIONS

An investigation of two variations of the gas generator method for calculating the thrust of the afterburning turbofan engines installed in the F-111A airplane yielded the following conclusions:

1. The gas generator method can be successfully applied to an afterburning turbofan engine. Based on two ground calibration tests, with two engines operating, net thrust accuracies of ± 2 percent can be achieved for most power settings.
2. An influence coefficient study showed that the overall accuracy of the calculation method based on nozzle total temperature and weight flow (TTW) was about equal to the accuracy of the method based on nozzle total pressure and area (PTA) at static conditions and was superior for in-flight conditions where, for military power,

estimated engine net thrust accuracy was approximately ± 3 percent for the TTW method and approximately ± 5 percent for the PTA method.

3. With either calculation method, additional errors in calculated thrust of as much as ± 2 percent could result from high inlet flow distortion.

4. The PTA method and the TTW method should both be used to calculate the thrust of an afterburning turbofan engine if accurate results are required.

Flight Research Center,
National Aeronautics and Space Administration,
Edwards, Calif., January 5, 1971.

APPENDIX

DEFINITION OF PARAMETERS

Distortion Parameter, K_D

The distortion parameter, K_D , is defined as follows:

$$K_D = \frac{\sum_{r=1}^n \left[\left(\frac{\Delta p}{p} \right)_r \left(\frac{d_o}{d_r} \right)_r \theta_r^- \right]}{\sum_{r=1}^n \left(\frac{d_o}{d_r} \right)}$$

where

r a particular ring of total pressure probes

$$\left(\frac{\Delta p}{p} \right)_r = \frac{p_{t_{av}} - p_{t_{min}}}{p_{t_{av}}} \times 100, \text{ in percent, for a particular ring}$$

$p_{t_{av}}$ average pressure per ring

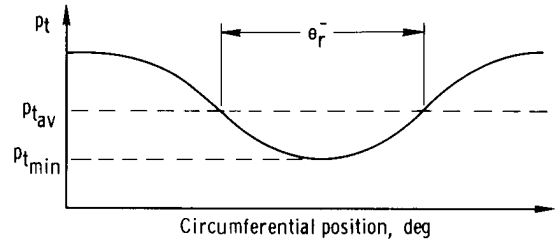
$p_{t_{min}}$ minimum pressure per ring

d_o outer diameter of duct

d_r diameter of a particular ring

θ_r^- circumferential extent of largest single pressure depression below $p_{t_{av}}$, in degrees, for a particular ring (See adjacent sketch.)

n number of measurement rings



Relative Distortion Parameter, D_r

The relative distortion parameter, D_r , is defined by the following equation:

$$D_r = \left(\frac{K_{D_{\text{off-design inlet}}}}{K_{D_{\text{cowl open}}}} \right)_{\text{same net thrust}}$$

APPENDIX

Influence Coefficient, C_i

The influence coefficient, C_i , is defined as follows:

$$C_{i(\text{parameter})} = \left(\frac{\Delta F_n}{F_n} \times 100 \right)_{+1 \text{ percent } \Delta(\text{parameter})}$$

REFERENCES

1. Waters, Mark H.; and Graham, Philip A.: Evaluation of an Exhaust Nozzle Traversing Rake System as an In-Flight Thrust Measuring Device for an Afterburning Turbofan Engine. NAPTC-ATD-150, Naval Air Propulsion Test Center (Trenton, N. J.), Nov. 1968.
2. Beeler, De E.; Bellman, Donald R.; and Saltzman, Edwin J.: Flight Techniques for Determining Airplane Drag at High Mach Numbers. NACA TN 3821, 1956.
3. Nugent, Jack: Lift and Drag of a Swept-Wing Fighter Airplane at Transonic and Supersonic Speeds. NASA Memo 10-1-58H, 1959.
4. Beaulieu, Warren; Campbell, Ralph; and Burcham, William: Measurement of XB-70A Propulsion Performance Incorporating the Gas Generator Method. J. Aircraft, vol. 6, no. 4, July-Aug. 1969, pp. 312-317.
5. Arnaiz, Henry H.; and Schweikhard, William G.: Validation of the Gas Generator Method of Calculating Jet-Engine Thrust and Evaluation of XB-70-1 Airplane Engine Performance at Ground Static Conditions. NASA TN D-7028, 1970.
6. Mechtly, E. A.: The International System of Units - Physical Constants and Conversion Factors. NASA SP-7012, 1969.
7. Humphrey, J. R., Jr.; and Fallon, J. F., Jr.: In-Flight Performance Determination for TF30-P-3 Engine. Rep. PWA-3106, Pratt & Whitney Aircraft, Sept. 1968.
8. Braithwaite, Willis M.; and Vollmar, William R.: Performance and Stall Limits of a YTF30-P-1 Turbofan Engine With Uniform Inlet Flow. NASA TM X-1803, 1969.
9. Werner, Roger A.; Abdelwahab, Mahmood; and Braithwaite, Willis M.: Performance and Stall Limits of an Afterburner-Equipped Turbofan Engine With and Without Inlet Flow Distortion. NASA TM X-1947, 1970.
10. Boytos, Joseph F.; and Pasela, Walter L.: Exhaust Nozzle Characteristics of a Pratt & Whitney Aircraft TF30-P-8 Turbofan Engine at Simulated Flight Conditions. NAPTC-ATD-186, Naval Air Propulsion Test Center (Trenton, N. J.), May 1970.